Wigner crystal in snaked nanochannels

O.V.Zhirov[1] and D.L.Shepelyansky[2]

[1]*Budker Institute of Nuclear Physics, 630090 Novosibirsk, Russia*
[2]*Laboratoire de Physique Théorique du CNRS (IRSAMC), Université de Toulouse, UPS, F-31062 Toulouse, France*

(Dated: February 7, 2011)

We study properties of Wigner crystal in snaked nanochannels and show that they are characterized by conducting sliding phase at low charge densities and insulating pinned phase emerging above a certain critical charge density. The transition between these phases has a devil's staircase structure typical for the Aubry transition in dynamical maps and the Frenkel-Kontorova model. We discuss implications of this phenomenon for charge density waves in quasi-one-dimensional organic conductors and for supercapacitors in nanopore materials.

PACS numbers: 05.45.Ac, 71.45.Lr, 82.47.Uv

The Wigner crystal [1] appears in a great variety of physical systems including electrons in two-dimensional semiconductor samples and one-dimensional (1D) nanowires (see review [2] and Refs. therein), electrons on a surface of liquid helium [3], cold ions in radio-frequency traps [4] and dusty plasma in laboratory or in space [5]. Effects of Coulomb interactions are clearly seen experimentally in nanowires [6, 7] and carbon nanotubes [8]. Also interaction effects for electrons in microchannels on a surface of liquid helium have been recently observed experimentally [9]. In view of this remarkable progress it is interesting to investigate sliding and conducting properties of the Wigner crystal in wiggled or snaked nanochannels. The interest to such studies goes back to the Little suggestion [10] on electron conduction in long spine conjugated polymers where he proposed an approach for synthesizing of organic superconductors. A modern overview discussion of this important suggestion is given in [11]. A schematic image of electron transport in such organic molecules is shown in Fig. 1a. According to this picture long molecules form wiggling channels which in principle can support electron transport along them. However, the Coulomb interactions between electrons are rather strong at such small scales and thus it is not obvious under what conditions a sliding of Wigner crystal along such channels is possible. This problem is related to the conduction properties of charge density waves (CDW) (see e.g. reviews [11, 12]). To study this phenomenon we choose a simple model of 1D snaked channel shown in Fig. 1b. There is no potential gradient along the channel but the channel walls are assumed to be very high so that electrons can move only along the channel.

In addition, the properties of Wigner crystal in snaked nanochannels are also useful for understanding of mechanisms of charge storage in electrochemical capacitors, or supercapacitors, which start to have important industrial applications [13, 14]. In these systems, charged ions are stored in nanopores at the surface of the carbon-activated material which has enormously large capacitance C going beyond the meanfield values given by the Helmholtz

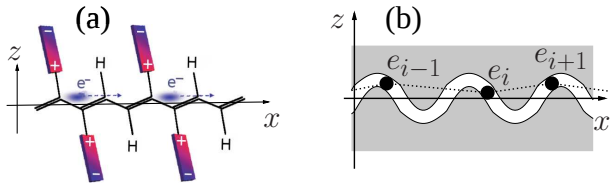

FIG. 1: (Color online) (a)A schematic image of the Little suggestion for electron transport in organic molecules (after [10, 11]). (b) A schematic image of electron Wigner crystal with charges e_i (points) sliding in a snaked sinusoidal nanochannel, dashed lines show force directions between nearby electrons.

theory [15, 16]. At nanoscale the wiggling of pores is definitely present that makes our studies very timely.

Due to sinusoidal channel wiggling the Wigner crystal moves in a certain effective periodic potential. The case of sliding of 1D Wigner crystal in a periodic energy potential was analyzed in [17] having in mind an example of ion chains in optical lattices. It was shown there that this problem can be locally reduced to the Frenkel-Kontorova model for a particle spring chain in a periodic potential [18] with particle positions described by the Chirikov standard map [19]. For a small amplitude of periodic potential the Wigner crystal with an incommensurate ion density can slide in an optical lattice but above a certain critical amplitude of potential the crystal is pinned by the lattice due to the Aubry analyticity breaking transition [20]. In the pinned phase the phonon spectrum has a gap for long wave excitations so that this regime corresponds to an insulating phase. This situation corresponds to a dynamical spin glass phase with exponentially many stable classical configurations being exponentially close to a ground state at a fixed electron density [17]. The Frenkel-Kontorova model is characterized by similar classical and quantum properties [21, 22]. At sufficiently large values of effective Planck constant a quantum instanton tunneling between these quasidegenerate configurations leads to a zero-temperature quantum phase transition due to which the quantum Wigner crystal becomes conducting [17]. In the following we show that the main elements of

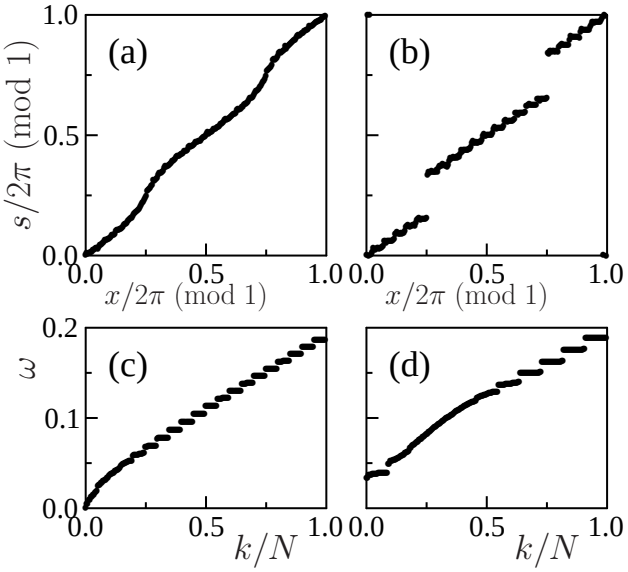

FIG. 2: (Color online) Hull function $s = h(x)$ (a,b) and phonon spectrum $\omega(k/N)$ (c,d) for incommensurate electron densities $\nu = N/L = 239/233$ (a,c) and $\nu = N/L = 244/233$ (b,d). Here $a = 1.2$.

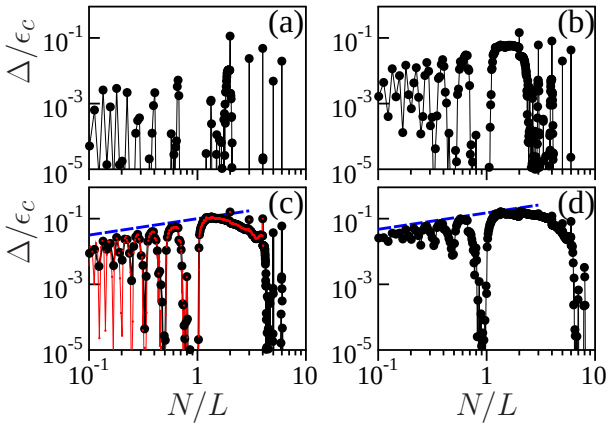

FIG. 3: (Color online) Dependence of the dimensionless phonon gap Δ/ϵ_c on the electron density $\nu = N/L$ for $a = 0.7(a)$, $1(b)$, $1.2(c)$, $1.5(d)$. Here $L = 89$ (black), 233 (gray/red). The straight line shows empirical dependence $\Delta/\epsilon_c \propto (N/L)^{1/2}$ for (c, d), where $\epsilon_c = 2\pi e^2\nu/\ell = \nu$ is the Coulomb energy.

this physical picture remain valid for the Wigner crystal in snaked nanochannels which are however characterized by enormously sharp changes of conducting properties.

We start our analysis from the case of classical electrons with Coulomb interactions moving in a snaked nanochannel shown in Fig. 1b. In this case the total system energy E is given by a sum over all Coulomb interactions. Due to strong nonlinearity of the system the minimal energy configurations should be find numerically using the methods described in [17, 20–22]. We take a finite number of electrons N for L periods of a channel of finite length. In numerical simulations we put the channel on a cylindrical surface in 3D with electron coordinates being $x_i = L\sin(s_i/L)$, $y_i = L\cos(s_i/L)$, $z = a\sin(s_i)$ where s_i is coordinate along channel for electron i. Thus the channel, filled by N electrons, wiggles in $z-$direction making L periodic oscillations along cylinder of radius L with periodic boundary conditions. The Coulomb energy of the system is

$$E = \sum_{j>i} 1/R(s_i, s_j) \qquad (1)$$

where $R(s_i, s_j)$ is the distance between two electrons. We find from geometry $R^2(s_i, s_j) = 4L^2\sin^2[(s_i - s_j)/2L] + a^2(\sin s_i - \sin s_j)^2$. Here we choose dimensionless units for charge e and length, so that the channel period length is $\ell = 2\pi$ and dimensionless amplitude of channel oscillations is a. In the limit of large L we have a channel wiggling in (x, z) plane. At $a = 0$ we have electrons on a circle.

The equilibrium static configurations are defined by the condition $\partial E/\partial s_i = 0$ with a minimal ground state energy configuration determined numerically by the standard methods [17, 20, 21]. Using these methods we also find the phonon spectrum $\omega(k)$ of small oscillations at the ground state. It is easy to see that the total energy E is invariant for a homogeneous shift of all electrons by δs when the distance between nearby electrons is $s_{i+1} - s_i = 2\pi m$ that corresponds to electron density $\nu = N/L$ with resonant rational values $\nu_m = 1/m$. Hence, at such a density the Wigner crystal can freely slide along the channel. For irrational density values the properties of sliding are much more tricky. An example is shown in Fig. 2 for two very close incommensurate densities ν. For $\nu = 239/233$ we have a smooth hull function $s_i = h(x_i)(mod 2\pi)$ with the gapless phonon spectrum $\omega \propto \omega_0 k/N$ at small wave numbers k/N. Here $x_i(mod 2\pi)$ are ground state electron positions at $a = 0$. The dimensional unit of frequency $\omega_0 = (e^2/(m(\ell/2\pi)^3))^{1/2}$ is expressed via the particle charge e, mass m and channel period ℓ, we omit it in the further dimensionless computations. This regime corresponds to the continues invariant Kolmogorov-Arnold-Moser (KAM) curves as it is discussed for the Frenkel-Kontorova model [17–21]. Here, the Wigner crystal can slide freely along the nanochannel. In contrast, for very close density $\nu = 244/233$ the hull function starts to have devil's staircase form, well known for the cantori regime in the Frenkel-Kontorova model. Here, the gap Δ appears in the phonon spectrum so that the crystal is pinned in the channel. This regime corresponds to the insulating phase.

The dependence of phonon gap Δ on electron density ν is shown in Fig. 3 for various values of channel deformation amplitude a. At small deformations the gap is zero for a large fraction of densities ν (Fig. 3a) and the crystal can slide freely along the channel. However, at larger deformations the gap disappears only in a vicinity

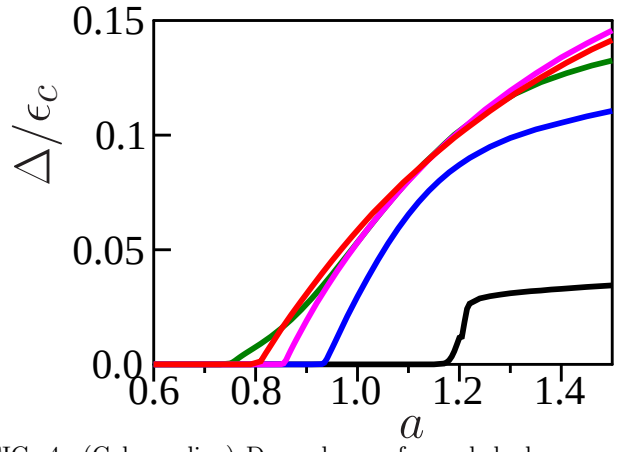

FIG. 4: (Color online) Dependence of rescaled phonon gap Δ/ϵ_c on channel deformation amplitude a at various values of electron density ν with the number of electrons $N = 241$ (black), 269(blue), 337 (magenta), 377 (red), 307 (green) (curves from right to left at $\Delta/\epsilon_c = 0.01$ respectively) at $L = 233$.

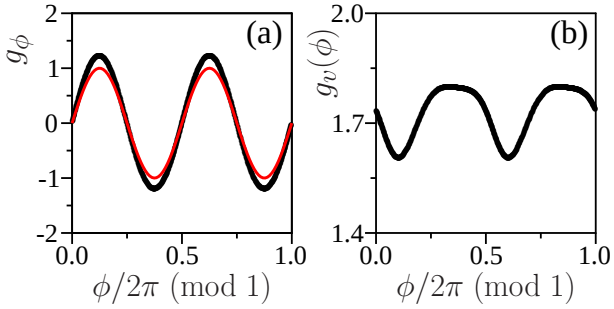

FIG. 5: (Color online) Map kick functions $g_\phi(\phi)$ (a) and $g_v(v)$ (b) obtained from the groundstate electron positions s_i in nanochannel (points), full red/gray curve in (a) shows the theoretical dependence from the map (2), see also text. Here N=377, L=233, $a = 0.5$.

of rational densities ν_m (Fig. 3b,c) and at strong deformation regime only narrow zero gap intervals remain around these density values (Fig. 3d). We note that our numerical data are obtained at rather large number of electrons N and channel periods L so that the dependence $\Delta(\nu)$ found numerically corresponds to the limit of infinite channel length. Indeed, the function $\Delta(\nu)$ remains practically unchanged with an increase of L (Fig. 3c). The global dependence of Δ on ν corresponds to frequency of small charge oscillations $\Delta \propto \nu^{3/2} \propto 1/\ell^{3/2}$, being in agreement with data of Fig. 3c,d.

A remarkable feature of the dependence $\Delta(\nu)$ is its very sharp variation with density ν and deformation a. The dependence is enormously sharp in a vicinity $\nu = 1$: for $\nu < 1$ there is crystal sliding in the channel while only slightly above $\nu = 1$, e.g. for $N/L = 1 + 11/233$, we obtain the insulating phase. This reminds a sharp change of conduction properties of organic materials with pressure [11] which effectively modifies ν and a values.

The dependence of phonon gap Δ on channel deformation a is shown in Fig. 4 for few density values ν. The gap changes smoothly with a for $a > a_c$ where a_c is a certain critical value of deformation which depends of density ν. For $a < a_c$ we find very sharp drop of Δ which becomes exponentially small, e.g. Δ drops by 5 orders of magnitude when a is decreased by a couple percents in a vicinity of a_c. Since simulations are done at a finite N this means that in the thermodynamic limit $\Delta = 0$ for $a < a_c$. We interpret these data in a way similar to the case of the Frenkel-Kontorova model [18, 20, 21]: for $a < a_c(\nu)$ we have an analytic invariant KAM curve with a rotation number corresponding to a given density, while for $a > a_c$ this curve is replaced by a cantori with a finite phonon gap and pinning of the crystal.

To understand in a better way the numerical results presented above we derive an approximate dynamical map which determines recursively the electron positions along the channel. The recursion is given by equilibrium conditions $\partial E/\partial s_i = 0$. Assuming that $a \ll 1$ we can expand R in a that, after keeping only nearest electron interactions, gives recursive relations between s_{i-1}, s_i, s_{i+1}. They can be presented in a form of dynamical map

$$\begin{aligned} \bar{v} &= v + 2a^2(1 - \cos\bar{v}) \sin 2\phi \,, \\ \bar{\phi} &= \phi + \bar{v} + a^2 \sin\bar{v} \cos 2\phi \,, \end{aligned} \qquad (2)$$

where $v = s_i - s_{i-1}$, $\phi = s_i$ are conjugated action-phase variables, bar marks their values after iteration. The map is implicit but symplectic (see e.g. [23]). To check its validity we use the values s_i obtained for the groundstate configuration and extract from them the kick function $g_\phi = \sin 2\phi$ from the values $\bar{v} - v = 2a^2 g_v(v) g_\phi(\phi)$ with $g_v(v) = 1 - \cos v$. Such a check shows that the map (2) indeed gives a good description of actual electron positions s_i up to moderate values of a (Fig. 5).

At small a the phase space of the map is covered by invariant KAM curves as it is shown in Fig. 6 (left). At larger a a single chaotic component covers a significant part of the phase space (Fig. 6 right). Locally the dynamics is approximately described by the Chirikov standard map with the chaos parameter $K \approx 4a^2(1 - \cos v)$. According to [19, 23] the KAM curves are destroyed at $K > 1$ that is in a good agreement with our numerical data of Fig. 3 where the KAM curve with the golden rotation number $\nu = 0.618...$ goes to the cantori regime approximately at $a \approx 0.4$. We note that at small charge density ν the parameter K is small $K \approx 2a^2\nu^2 \ll 1$ that corresponds to the KAM regime and a conducting phase of Wigner crystal in agreement with the data of Fig. 3.

Of course, the map description is valid only up to moderate a values. At $a > 1$ the expansion in a is no more valid that explains the asymmetry in the dependence for $\Delta(\nu)$ at $\nu < 1$ and $\nu > 1$ which is absent in the approximate map (2) but is clearly seen in Fig. 3. Further studies are required to obtain a map description at large values of deformation a.

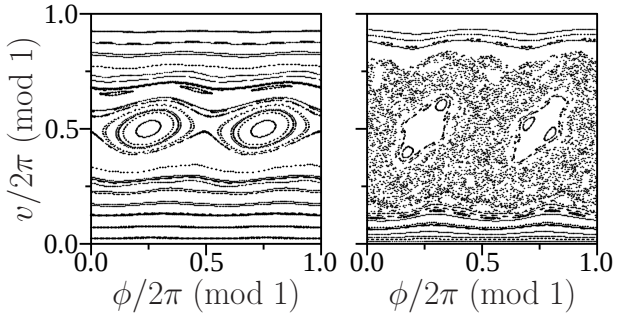

FIG. 6: (Color online) Poincare section for the dynamical map (2) at $a = 0.25$ (left panel), 0.5 (right panel).

Our studies determined conditions of sliding and pinning of the Wigner crystal in snaked nanochannels. Here, we performed only classical analysis. According to results of [17] the quantum effects are weak if the dimensionless effective Planck constant $\hbar_{eff} = (2\pi\hbar^2/me^2\ell)^{1/2}$ is small. This is definitely the case for supercapacitors with $\ell/2\pi \sim 1nm$, large ion mass $m \sim 4 \cdot 10^4 m_e$ compared to electron mass m_e, that gives $\hbar_{eff} \sim 10^{-3}$. The charge storage process in this case starts with small charge density values ν where the ions slide easily in nanochannels since the gap Δ is practically absent there (see Fig. 3). However, with the increase of ν ions form the Wigner crystal which is pinned inside the nanopores at large ν values. We think that this is the physical mechanism behind the charge process of electrochemical capacitors studied in [13, 14]. We note that the energy of pinned Wigner crystal can be estimated as $W_W \sim Sde^2/\epsilon(\ell/2\pi)^4$, where S is the surface area, d is the deepness of nanopore layer on the surface and ϵ is the dielectric constant. For typical parameters $\epsilon = 5$, $\ell/2\pi = 1nm$, $d = 1\mu m$ we obtain $W_W/S \approx 5 \cdot 10^{-3} J/cm^2$. It is natural to assume that a part of this energy can be used during recharging process that makes it comparable with the surface energy density reached in supercapacitors with $W/S \sim 10^{-3} J/cm^2$ at maximal capacitance per area $C \approx 400\mu F/cm^2$ and voltage $U \sim 2V$ [13, 14]. We note that our estimate gives an increase of W_W with a decrease of nanopore size ℓ that qualitatively corresponds to the behavior observed experimentally (see e.g. Fig.3a in [14]). At the above parameters the typical pinning frequency is $\omega_0\Delta/2\pi \sim 50GHz$ so that the Wigner crystal should be sensitive to microwave radiation in this frequency range.

In contrast, for CDW in organic conductors [11] we have $m \sim m_e$, $\ell/2\pi \sim 3\mathring{A}$ that gives $\hbar_{eff} \sim 0.5$ so that quantum effects can play an important role. Further studies are required to analysis quantum properties of crystal sliding but we expect that they will have similarities with the quantum Wigner crystal in a periodic potential [17] and the quantum Frenkel-Kontorova model [22]. The classical pinned phase should correspond to the insulator phase, while we expect that the classical sliding phase may correspond to the superconducting regime in the quantum case. Indeed, the sliding phase has a linear dispersion law $\omega(k)$ that can be similar to the situation in superfluid phase. The sharp transitions from conducting to insulating phase with charge density variation are well pronounced in the classical regime and are expected to be present also in the quantum case. This can be at the origin of high sensitivity of organic conductors to pressure. Further studies should shed more light on the quantum properties of Wigner crystal in snaked nanochannels and organic molecular chains. It would be very interesting to study such effects experimentally creating artificial snaked channels with electrons on a surface of liquid helium [9].

This research is supported in part by ANR PNANO project NANOTERRA.

[1] E. Wigner, Phys. Rev. **46**, 1002 (1934).
[2] J.S. Meyer and K.A. Matveev, J. Phys. C.: Condens. Mat. **21**, 023203 (2009).
[3] Y. Monarkha and K. Kono, *Two-Dimensional Coulomb Liquids and Solids*, Springer-Verlag, Berlin (2004).
[4] D.H.E.Dubin and T.M. O'Neil, Rev. Mod. Phys. **71**, 87 (1999).
[5] V.E. Fortov, A.V. Ivlev, S.A. Khrapak, A.G. Khrapak, and G.E. Morfill, Phys. Rep. **421**, 1 (2005).
[6] O.M. Auslaender *et al.* Science **308**, 88 (2005).
[7] Y. Jompol *et al.* Science **325**, 597 (2009).
[8] V.V. Deshpande *et al.* Science **323**, 106 (2009).
[9] D.G. Rees *et al.* Phys. Rev. Lett. **106**, 026803 (2011).
[10] W.A. Little, Phys. Rev. A **134**, 1416 (1964); Sci. Am. **212**, 21 (1965).
[11] D. Jérome, *Historical Approach to Organic Superconductivity*, in *The Physics of Organic Superconductors and Conductors* A.Lebed (Ed.), p.3, Springer-Verlag, Berlin (2008).
[12] R.E. Thorne, Phys. Today **5**, 43 (1996).
[13] P. Simon and Y. Gogotsi, Nat. Mater. **7**, 845 (2008).
[14] P. Simon and Y. Gogotsi, Phil. Trans. R. Soc. A **368**, 3457 (2010).
[15] B. Skinner, M.S. Loth, and B.I. Shklovskii, Phys. Rev. Lett. **104**, 128302 (2010).
[16] B. Skinner, T. Chen, M.S. Loth, and B.I. Shklovskii, arXiv:1101.1064[cond-mat.mtrl-sci] (2011).
[17] I. Garcia-Mata, O.V. Zhirov and D.L. Shepelyansky, Eur. Phys. J. B **41**, 325 (2007).
[18] O.M. Braun and Yu.S. Kivshar, *The Frenkel-Kontorova Model: Concepts, Methods, Applications*, Springer-Verlag, Berlin (2004).
[19] B.V. Chirikov, Phys. Rep. **52**, 263 (1979).
[20] S. Aubry, Physica D **7**, 240 (1983).
[21] O.V.Zhirov, G.Casati and D.L.Shepelyansky, Phys. Rev. E **65**, 026220 (2002).
[22] O.V.Zhirov, G.Casati and D.L.Shepelyansky, Phys. Rev. E **67**, 056209 (2003).
[23] A.J. Lichtenberg and M.A. Lieberman, *Regular and chaotic dynamics*, Springer, Berlin (1992).